Journal of Hazardous Materials 499 (2025) 140255

Contents lists available at ScienceDirect

Journal of Hazardous Materials

journal homepage: www.elsevier.com/locate/jhazmat

Polytetrafluoroethylene (PTFE, Teflon) microplastics and nanoplastics induce oxidative stress, mitochondrial damage, and genotoxicity in human intestinal cells

Doaa Abass [a,b,*], Mohamed Alaraby [a,b], Elham Farghal Elkady [c], Michelle Morataya-Reyes [a], Gooya Banaei [a], Joan Martín-Pérez [a], Laura Rubio [a], Irene Barguilla [a], Ricard Marcos [a], Alba Hernández [a], Alba García-Rodríguez [a,*]

[a] Group of Mutagenesis, Department of Genetics and Microbiology, Faculty of Biosciences, Universitat Autònoma de Barcelona, Cerdanyola del Vallès, 08197, Spain
[b] Zoology Department, Faculty of Science, Sohag University, Sohag 82524, Egypt
[c] Plant Protection, Institute of Agricultural Research Center, Sohag, Egypt

HIGHLIGHTS

- Polytetrafluoroethylene micro/nanoplastics affect human intestinal cells.
- Both undifferentiated and differentiated (barrier) cells were affected.
- Smaller particles and longer exposure enhanced the induced harmful effects.
- Mitochondrial dysfunction, genotoxicity, and inflammation was induced.
- Low risk, by assuming chemical inertness and low release, is discarded.

GRAPHICAL ABSTRACT

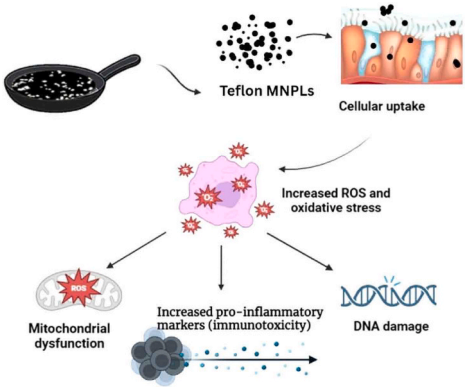

ARTICLE INFO

Keywords:
Teflon™
Micro/nanoplastics
Human
Intestinal barrier
Oxidative stress
Genotoxicity
Mitochondrial damage

ABSTRACT

Polytetrafluoroethylene (PTFE, Teflon™), widely used in non-stick cookware, can degrade into micro- and nanoplastics (MNPLs). This raises concerns about human exposure, which remain largely unexplored. In the present study, we used physiologically relevant *in vitro* intestinal monoculture and co-culture models (Caco-2/HT29-MTX) to systematically assess the effects of PTFE-MNPLs (~250 nm and ~2 μm) at concentrations of 50–200 μg/mL over 24–48 h. PTFE-MNPLs, particularly nanosized particles, readily entered both differentiated and undifferentiated cells. They interacted with nuclear membranes and mitochondria, inducing structural and physiological disturbances without significantly affecting cell viability. These interactions led to mitochondrial damage and triggered inflammation, oxidative stress, and DNA damage. The severity of these effects increased with particle size, dose, and exposure duration. These findings challenge the assumption that PTFE particles are

* Correspondence to: Group of Mutagenesis, Department of Genetics and Microbiology, Faculty of Biosciences, Universitat Autònoma de Barcelona, Campus of Bellaterra, Cerdanyola del Vallès (Barcelona), 08193, Spain.
E-mail addresses: doaa_gad@science.sohag.edu.eg (D. Abass), alba.garcia.rodriguez@uab.cat (A. García-Rodríguez).

https://doi.org/10.1016/j.jhazmat.2025.140255
Received 2 August 2025; Received in revised form 30 September 2025; Accepted 23 October 2025
Available online 26 October 2025

biologically inert, highlighting hazards arising from their physical interactions, especially at the nanoscale. Given the relevance of the co-culture in vitro model of intestinal barrier to human intestinal physiology, the results underscore potential intestinal health risks from PTFE-MNPL exposure. Future studies should focus on chronic, low-dose exposures to elucidate the specific cellular pathways activated by PTFE-MNPL exposure.

1. Introduction

Plastic production has increased exponentially in recent decades, resulting in widespread waste and pervasive environmental pollution [1]. The degradation of plastics in the environment generates micro- and nanoplastics (MNPLs), emerging contaminants capable of entering organisms, crossing biological barriers, and disrupting tissue structure and function [2,3]. As sources of MNPLs continue to expand, human exposure, and associated health risks, are increasing, particularly through direct interactions with contaminated materials. Daily exposure can occur via food, especially when using plastic-related cooking tools, yet the potential risks of these exposures have long been underestimated. For instance, food containers made from polypropylene and polystyrene can release significant amounts of microplastics (100,000–260,000 particles), particularly under freezing or heating conditions [4].

Polytetrafluoroethylene (PTFE), commonly known as Teflon™, is a potential emerging source of MNPLs, yet it has received little research attention [5]. PTFE is widely used due to its non-stick properties, thermal resistance, low friction, and chemical inertness [6,7]. Although long considered stable, recent studies reveal that PTFE-coated cookware can release thousands to millions of particles during routine use, including brief cooking sessions or minor scratches [8]. Many of these particles can transfer to food or persist on cookware surfaces, posing a chronic ingestion risk [9]. Recently, PTFE microplastics (300 nm–5 μm) have been shown to impair embryonic development, inducing mortality, vascular defects, and neural abnormalities [10]. These findings have sparked renewed concern about the safety of PTFE-based kitchen products, especially in the absence of comprehensive toxicological evaluation [11].

MNPLs have been found to cross biological barriers, such as the intestinal and pulmonary epithelium, and accumulate in different organs, tissues, bodily fluids, and excreta [12,13]. Their presence in the gut can disrupt intestinal health and potentially induce microbial dysbiosis [14]. *In vitro* intestinal models have become essential tools for studying MNPLs toxicity via oral exposure, the primary route of human intake [15–17]. Recent studies using Caco-2 and HT29-MTX co-cultures demonstrate their ability to simulate intestinal barrier responses to MNPLs released from food containers. Observed effects include oxidative stress, mitochondrial dysfunction, membrane damage, and altered gene expression [18–20]. This evidence underscores the suitability of these models for investigating MNPL impacts across a wide array of biological pathways.

The present study aims to evaluate the toxicological effects of PTFE-derived MNPLs using undifferentiated and differentiated Caco-2/HT29-MTX co-cultures, investigating MNPL internalization, interactions with cellular components, and the influence of particle size, shape, and morphology. The study further assesses the impact of PTFE-MNPLs on cellular homeostasis, including various cellular and physiological pathways. Through this approach, it provides preliminary mechanistic insights into the harmful effects of PTFE-MNPLs and addresses critical knowledge gaps regarding their potential impact on intestinal health, which have not been thoroughly examined previously.

2. Materials and methods

2.1. Physicochemical characterization and preparation of PTFE-MNPLs dispersions

Two distinct commercial types of PTFE-MNPLs were used in this study: micro-sized particles (PTFE-MPLs) obtained from Nanoshel (UK) and nano-sized particles (PTFE-NPLs) from Sigma-Aldrich (USA). Particle characterization including size, morphology, shape, and dispersity was performed using dynamic light scattering (DLS; Malvern Zetasizer Nano-ZS), transmission electron microscopy (TEM; HITACHI H-7000, 125 kV), and scanning electron microscopy (SEM; Zeiss Merlin). Chemical composition was confirmed via Fourier-transformed infrared spectroscopy (FTIR; Hyperion 2000, Bruker). To ensure uniform dispersion, PTFE particles were suspended in 40 mL Milli-Q water at 15 mg/mL and subjected to sonication (400 W, 10 % amplitude) in an ice-water bath for 16 min, followed by magnetic stirring at 800 rpm for 2 h to prevent sedimentation due to their hydrophobic nature. Aliquots were stored at −80 °C for future use.

2.2. Intestinal cell models and culture conditions

Two human colon adenocarcinoma cell lines, Caco-2 and HT29-MTX, were used as undifferentiated monocultures or differentiated co-cultures forming an *in vitro* intestinal barrier. Undifferentiated models lack intestinal barrier complexity, while differentiated co-cultures mimic the epithelium with polarized Caco-2 cells and mucus-secreting HT29-MTX cells. Caco-2 cells were initially kindly provided by Dr. Isabella de Angelis (ISS, Italy), and HT29-MTX cells were purchased from ATCC (USA). Both lines were cultured in high-glucose DMEM (without sodium pyruvate), supplemented with 10 % FBS, 1 % NEAA, 1 % Amphotericin B, and 2.5 μg/mL Plasmocin. Cells were maintained at 37 °C in a humidified 5 % CO_2 atmosphere and subcultured weekly at 70–80 % confluency using 1 % trypsin-EDTA. Undifferentiated cells were seeded at 1.7×10^5 cells/well for 24 h, while differentiated co-cultures (Caco-2:HT29-MTX, 90:10) were grown on 1.12 cm^2 Transwell® inserts for 21 days with bi-daily media changes to form a full barrier [21].

2.3. Cell viability studies

Cells (undifferentiated monocultures or differentiated co-cultures) were exposed to PTFE-MNPLs at concentrations of 0, 50, 100, and 200 μg/mL for 24 and 48 h. PTFE-MNPLs that were stored at –80 °C were thoroughly vortexed prior to use to ensure proper dispersion and prevent particle agglomeration. After exposure, cells were washed with PBS, detached with trypsin-EDTA, diluted in ISOTON (1:100), and viable cells were counted using a Coulter counter. Cell viability was quantified using the Z™ Series Coulter Counter (Beckman Coulter Inc., CA, USA). Viability data for each treatment condition represents the mean of three independent experiments, each performed in triplicate.

2.4. Cell internalization by TEM and confocal imaging

Internalization of PTFE-MNPLs was examined by TEM and confocal microscopy. Undifferentiated Caco-2, HT29-MTX, and differentiated co-cultures were exposed to 200 μg/mL PTFE-MNPLs for 48 h to facilitate visualization. For TEM, cells were fixed, resin-embedded, sectioned, stained, and imaged using a HITACHI H-7000 (125 kV). For confocal microscopy, PTFE-MNPLs were fluorescently labeled with iDye PolyPink [22], and after exposure, cells were counterstained for nuclei and membranes before imaging with a Leica TCS SP5. Images were processed with Fiji and Imaris software. The complete protocol is described in the supplementary material.

2.5. Barrier integrity by TEER measurements

Barrier integrity was assessed by measuring TEER using a Millicell-ERS volt/ohm meter. Barriers were exposed to PTFE-MPLs or PTFE-NPLs (0–200 μg/mL) for 24 and 48 h. At each 24 h interval, inserts were washed with PBS, fresh DMEM was added, and TEER was measured at three points per insert. Values were averaged from three independent experiments and normalized using TEER ($\Omega \cdot cm^2$) = [Ω(cell insert) − Ω(cell-free insert)] × 1.12 cm^2.

2.6. Inflammatory response

The inflammatory response level was quantified in both undifferentiated Caco-2 and HT29-MTX cells and differentiated Caco-2/HT29-MTX co-culture using the Human IL-8 Conferma™ ELISA Kit (Millipore Sigma). Cells were exposed to PTFE-MNPLs at concentrations 0–200 μg/mL for 24 or 48 h. Interleukin-8 (IL-8) levels were quantified in cell culture supernatants as per the manufacturer's instructions, and absorbance was measured at 450 nm using a POLARstar plate reader.

2.7. Mitochondrial membrane potential assay

Mitochondrial membrane potential in undifferentiated and differentiated Caco-2/HT29-MTX cells was assessed using the MitoProbe™ TMRM assay following 48 h exposure to 200 μg/mL PTFE-MNPLs. Cells were washed twice with PBS, trypsinized, centrifuged, and resuspended in PBS. TMRM fluorescence, reflecting mitochondrial membrane potential (Δψm), was measured by flow cytometry (CytoFLEX, Beckman Coulter, USA) at 561/585 nm excitation/emission. A total of 10,000 cells per sample were analyzed, and data were processed using CytExpert software.

2.8. Production of intracellular reactive oxygen species

Intracellular ROS levels were measured in undifferentiated Caco-2 and HT29-MTX cells, as well as in differentiated Caco-2/HT29-MTX co-cultures, using the dihydroethidium (DHE) assay kit (Abcam plc.). Cells were exposed to PTFE-MNPLs (0–200 μg/mL) for 24 or 48 h, washed, trypsinized, and stained with 10 μM DHE at 1×10^6 cells/mL for 30 min at 37 °C. After staining, cells were washed, resuspended in PBS, and kept on ice. Viability was assessed using Via-Probe™ Red, and flow cytometry was performed on ≥ 20,000 live cells per sample, with 100 μM Antimycin A-treated cells serving as a positive control.

2.9. Genotoxic and oxidative DNA damage by the comet assay

Genotoxicity was assessed in undifferentiated Caco-2, HT29-MTX, and differentiated co-cultures using the alkaline comet assay following PTFE-MNPL exposure (0–200 μg/mL, 24–48 h). Oxidative DNA damage in the barrier model was further evaluated with formamidopyrimidine-DNA glycosylase (FPG). Samples were electrophoresed, stained with SYBR Gold, and DNA damage quantified as % tail DNA in 100 nuclei/sample using Komet 5.5 software. Oxidative damage was calculated as the difference between FPG-treated and untreated samples. Potassium bromate (5 mM) and methyl methanesulphonate (2.5 mM) were used as positive controls. The complete protocol is described in the supplementary material.

2.10. Statistical analysis

All experiments were performed with at least two independent biological replicates, each containing a minimum of three technical replicates per treatment. Data are presented as mean ± standard error of the mean (SEM). Normality of the data was assessed using the D'Agostino-Pearson omnibus and Shapiro-Wilk tests, both conducted in GraphPad Prism version 9 (GraphPad Software, San Diego, CA, USA). For normally distributed data, statistical differences between groups were evaluated using one-way or two-way ANOVA, followed by Tukey's or Dunnett's post hoc tests as appropriate. Statistical significance was defined as $P \leq 0.05$.

3. Results and discussion

3.1. Physicochemical characterization of PTFE-MNPLs

Physicochemical characteristics are critical determinants of the toxicological profile of materials at the micro- and nanoscale. Accordingly, both PTFE types used in this study were extensively characterized (Fig. 1a–i). Microscopies analysis using SEM and TEM images revealed two distinct categories of PTFE-MNPLs: larger, irregular, and heterogeneous particles (Fig. 1a, c), and smaller, well-dispersed, homogeneous, nearly spherical particles (Fig. 1b, d). Particle size measurements further supported this distinction, with the first type in the microscale range (1979.5 ± 1227.6 nm; Fig. 1e) and the second in the nanoscale range (249.2 ± 59.2 nm; Fig. 1f). For clarity, the microscale particles are hereafter referred to as PTFE-MPLs, and the nanoscale particles as PTFE-NPLs.

Dynamic light scattering (DLS) further supported these findings, showing a broader distribution for PTFE-MPLs with a Z-average of 9113 ± 2023 nm and a polydispersity index (PDI) of 0.94 ± 0.11 (Fig. 1g). However, PTFE-NPLs had a mean diameter of 486.6 ± 20.3 nm and a narrower PDI of 0.52 ± 0.01, suggesting higher uniformity and greater monodispersed (Fig. 1g). The high PDI observed for PTFE-MPLs and the moderate PDI for PTFE-NPLs indicate the degree of heterogeneity, which increases with higher PDI values, and this finding is consistent with the morphological observations [23]. Although DLS measurements indicated that both PTFE-MPLs and PTFE-NPLs tend to aggregate in solution, the particles were well dispersed during treatment to minimize aggregation prior to exposure. Notably, previous studies have shown that the hydrodynamic diameter of particle agglomerates does not affect their biological impacts, such as the induction of DNA damage [24].

Fourier-transform infrared spectroscopy (FTIR) analysis confirmed the chemical identity of both particle types. Prominent stretching vibrations at approximately 1200 cm^{-1} and 1150 cm^{-1} (Fig. 1h, i) matched the characteristic spectral profile of PTFE, confirming that despite morphological and size differences, both PTFE-MPLs and PTFE-NPLs share the same fluoropolymer composition and chemical stability [7]. Although PTFE is traditionally considered chemically inert, its physical properties, particularly size and morphology, can strongly influence biological interactions and toxicity. Smaller PTFE particles, with higher surface-area-to-volume ratios, are more likely to be internalized and exhibit increased reactivity compared to larger ones. However, to date, few studies have examined the toxicological effects of PTFE-MNPLs using either *in vitro* or *in vivo* models, as recently reviewed [25].

3.2. Cell viability

In this study, no significant cytotoxic effects were observed for any of the PTFE-MNPLs treatments across the range of concentrations from 0 to 200 μg/mL and at any exposure duration (24 and 48 h) in either undifferentiated monoculture of Caco-2, HT29-MTX and differentiated intestinal co-culture model, Caco-2/HT29-MTX barrier (Fig. 2).

Studies indicate that PTFE-MNPLs exhibit low toxicity. In rats, dietary exposure to PTFE particles (5–50 μm; 0–2000 mg/kg) did not produce any noticeable changes in clinical signs, organ pathology, or body weight [26]. Likewise, the marine gastropod *Littorina brevicula* showed no adverse effects following exposure to PTFE (0.1–10 μm; 4 mg/cm^2) [27]. Consistent with these findings, no significant cytotoxicity was observed *in vitro* for PTFE-MNPLs (0–200 μg/mL; 24–48 h) in undifferentiated Caco-2 and HT29-MTX monocultures or in differentiated Caco-2/HT29-MTX co-cultures. However, the potential effects of PTFE-MNPLs remain poorly understood and warrant further

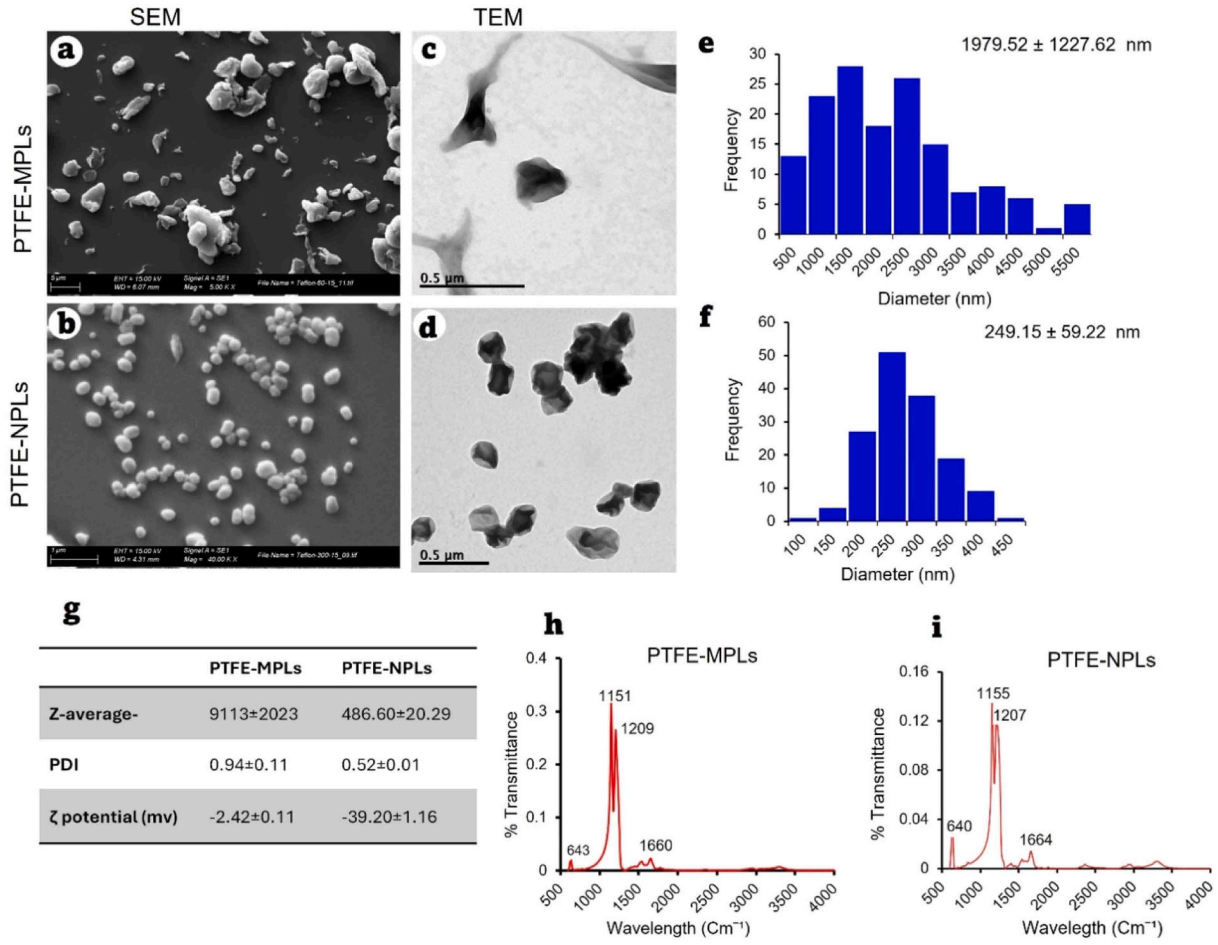

	PTFE-MPLs	PTFE-NPLs
Z-average-	9113±2023	486.60±20.29
PDI	0.94±0.11	0.52±0.01
ζ potential (mv)	-2.42±0.11	-39.20±1.16

Fig. 1. Physicochemical characterization of PTFE-MNPLs. Representative SEM (a, b) and TEM (c, d) images of both PTFE-MNPL types are shown. Size distributions of PTFE-MPLs and PTFE-NPLs (e, f), measured using ImageJ, revealed average sizes of 1979.5 ± 1227.6 nm and 249.2 ± 59.2 nm, respectively. Hydrodynamic size and zeta potential of both PTFE-MNPLs are shown in (g). FTIR spectra of PTFE-MNPLs (h, i) indicate the functional groups present in their chemical composition.

investigation. Their impact may not be limited to a reduction in cellular function; underlying physiological and pathological changes should also be assessed to fully elucidate their effects.

3.3. Cellular internalization

The ability of MNPLs to penetrate biological barriers is essential for risk assessment. It provides insight into the physiological and histopathological pathways they may affect. There is a need to study less-explored plastics across nano- and micrometre scales. Fluorescent labelling can help track their internalization in biological systems [28]. Mechanisms of internalization have been studied for polymers such as polystyrene (PS), polylactic acid (PLA), and polyethylene terephthalate (PET) using *in vitro* and *in vivo* models [29–31]. Most studies on microplastic uptake have focused on spherical, monodisperse PS particles, with little investigation into the effects of particle surface, shape, or material [32]. Research on PTFE-MNPLs is still in its early stages. Little is known about their interaction with biological barriers, especially the intestine, which is a primary route of internalization.

Imaging confirmed the internalization of both PTFE-MNPLs by intestinal epithelial cells. At 200 µg/mL, TEM and confocal microscopy revealed widespread intracellular localization of PTFE-NPLs, particularly around the nucleus, in close association with the nuclear membrane, and in some cases within mitochondria (Fig. 3). PTFE-MPLs were also internalized but to a lesser extent, appearing mainly near the nucleus or within the cytoplasm of barrier cells (Fig. 4). These findings highlight a clear size-dependent uptake, with nanoscale particles exhibiting greater penetrability than microscale counterparts.

The subcellular localization of PTFE-NPLs aligns with prior observations of nanoplastics, such as polystyrene, accumulating near mitochondria in enterocytes and other cell types [33]. Such interactions have been linked to mitochondrial morphological alterations and potential functional impairment [34]. The higher uptake of PTFE-NPLs compared to PTFE-MPLs underscores the greater biological reactivity of nanoscale plastics, whose small size and large surface-to-volume ratio facilitate internalization and intracellular transport [35]. These results highlight that particle size is a critical determinant of organelle-level interactions. This factor should be carefully considered when evaluating the toxicological risks of MNPLs, particularly for PTFE, which has not been thoroughly addressed.

On the other hand, a lower distribution of PTFE particles, irrespective of size, was observed in well-differentiated intestinal barriers compared with undifferentiated monocultures (Caco-2 and HT29-MTX). This reduced uptake is likely attributable to the differentiated state of the cells, which feature an apical brush-border structure, mature tight junctions, and a well-developed mucus layer [36]. Alaraby et al. [37] reported that, in *Drosophila* larvae, while some particles like CeO_2-NPs were able to penetrate the intestinal barrier, others remained in the lumen, attached to the peritrophic membrane. Together, these characteristics provide critical physical and biochemical protection that limits particle penetration. However, our findings are consistent with previous reports on other MNPLs, where nanoparticles were shown to be more readily internalized by undifferentiated or simpler epithelial models and to exhibit greater translocation efficiency than larger microparticles [38,

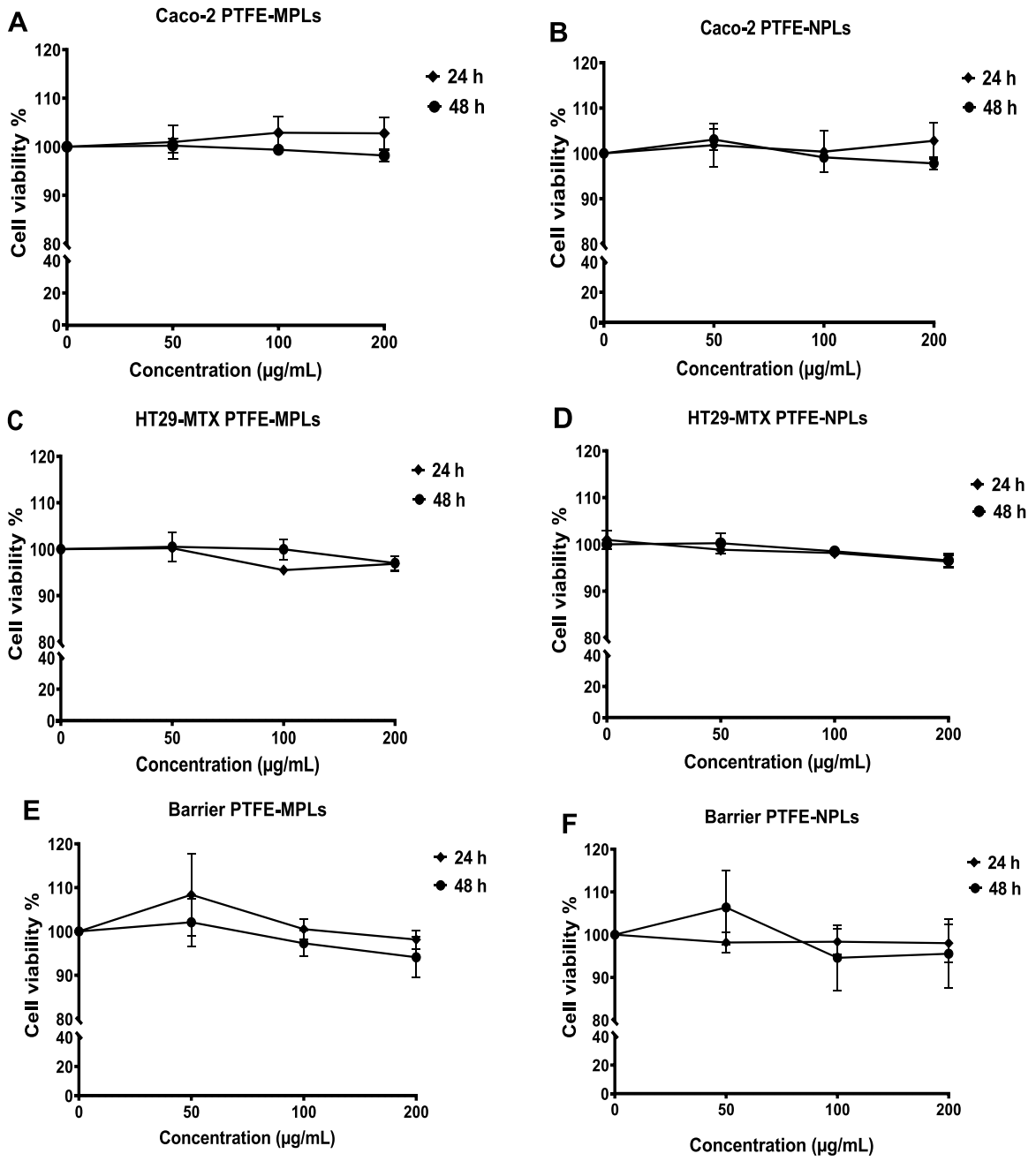

Fig. 2. Cell viability. Undifferentiated Caco-2 (A, B) and HT29-MTX monocultures (C, D), and the differentiated Caco-2/HT29-MTX co-culture barrier model (E, F) were exposed to PTFE-MNPLs (0, 50, 100, and 200 µg/mL) for 24 and 48 h. Cell viability is presented as a percentage relative to the negative control. Data are expressed as mean ± SEM and were analysed using one-way ANOVA followed by Dunnett's post-test. No significant effects were detected.

39].

3.4. *Effect of PTFE-MNPLs on the intestinal barrier integrity*

Intestinal barrier permeability can be compromised by MNPLs via disruption of tight junctions and weakening of ZO-1 proteins. TEER measurements provide an indicator of barrier integrity and potential adverse effects. Exposure to PLA-NPLs increased barrier permeability, suggesting epithelial damage [40].

After 21 days, the intestinal barrier was fully established, with baseline TEER values averaging 526 Ω·cm^2, confirming barrier integrity and tight junction formation [41]. Exposure to PTFE-MNPLs (0–200 µg/mL) maintained stable TEER values after 24 h (Fig. 5A). At 48 h, a slight decrease in cell viability was observed at 50–100 µg/mL, whereas a significant reduction occurred at 200 µg/mL, particularly for PTFE-NPLs (Fig. 5B), indicating a dose-, size-, and time-dependent effect. These findings align with our internalization data, showing higher uptake of PTFE-NPLs compared with PTFE-MPLs (Figs. 3–4). Previous studies also reported similar trends, such as TEER reductions following TiO_2-NPs exposure in a time- and shape-dependent manner [36]. Greater nanoparticle internalization may therefore contribute to subtle barrier dysfunction. Supporting this, PET microplastics can exacerbate PFOA toxicity by increasing cellular accumulation and inhibiting ZO-1 proteins [41]. TEM imaging revealed reduced tight junction density in barriers exposed to both PTFE-MPLs and PTFE-NPLs compared with controls (Fig. S1), indicating structural disruption. Tight junction integrity is vital for epithelial barrier function, with zonula occludens (ZO) proteins linking transmembrane junction components to the

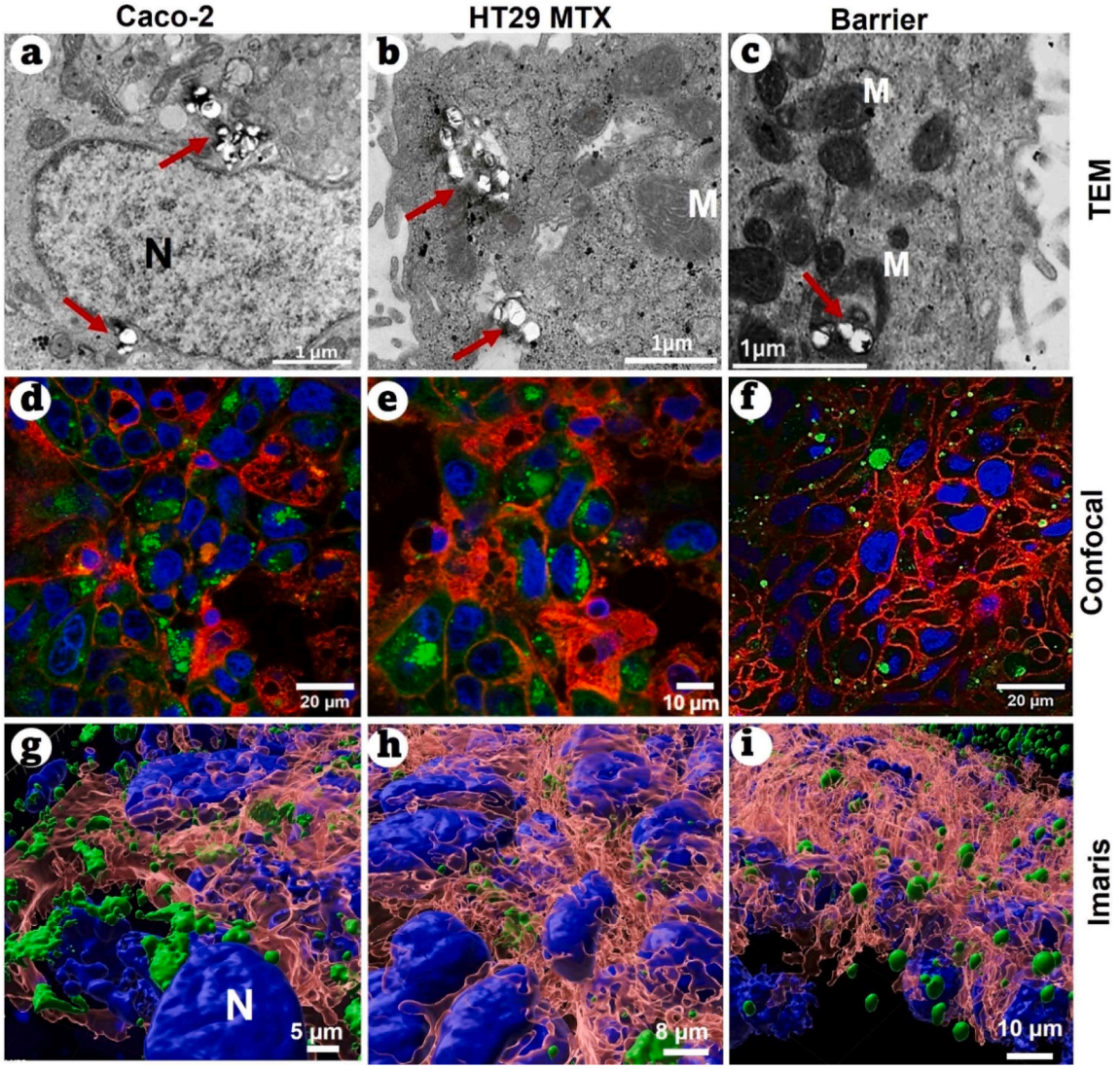

Fig. 3. Internalization of PTFE-NPLs (250 nm) after 48 h exposure in intestinal epithelial models. TEM images (a–c) show PTFE-NPLs uptake in Caco-2 cells (a), HT29-MTX cells (b), and the Caco-2/HT29-MTX co-culture barrier (c). Red arrows indicate endocytosed PTFE-NPLs within different cellular compartments. (N) denotes the nucleus; (M) denotes mitochondria. Confocal microscopy (d–i) confirms the intracellular localization of PTFE-NPLs (green), and 3D Imaris reconstructions (g–i) of the confocal images illustrate their spatial distribution.

cytoskeleton and regulating signalling pathways involved in inflammation, tissue repair, and tumorigenesis [42]. These findings raise questions about the physiological pathways affected by PTFE-MNPLs exposure, stemming from widespread particle distribution and apparent structural alterations.

3.5. *Pro-inflammatory effects of PTFE-MNPLs on intestinal epithelial models*

The capacity of MNPLs to induce inflammation is a critical concern, as it highlights potential hazard pathways and may help elucidate the mechanisms leading to deleterious biological responses. PS-NPs activate NF-κB/NLRP3 signalling, elevate IL-1β and IL-18, and recruit immune cells in the intestine, while downregulating tight junction proteins (Claudin-1, Occludin, ZO-1). This increases permeability, triggers inflammation and intestinal barrier disruption [43]. To address the immunotoxic potential of PTFE-MNPLs, IL-8 secretion was measured in differentiated Caco-2/HT29-MTX co-cultures (Fig. 6). After 24 h, no significant changes were observed (Fig. 6A). After 48 h, a modest but statistically significant increase (10–15 %) in IL-8 was observed (Fig. 6B). PTFE-NPLs showed a clear concentration-dependent response. PTFE-MPLs induced a slight increase only at the lowest concentration. This suggests that cumulative nanoparticle internalization and sustained intracellular interactions may activate downstream pro-inflammatory signalling pathways. Although data on PTFE-related effects are limited, PTFE-MPLs have been shown to induce oxidative stress, inflammation, and cytokine alterations in human cells [44,45]. Inflammatory responses from MNPLs are associated with age-related diseases and may accelerate cellular senescence via mitochondrial dysfunction, impaired autophagy, and DNA damage [46].

3.6. *Intracellular ROS production and mitochondrial membrane potential*

PTFE-MNPLs can induce structural and pathological alterations through their internalization, particularly affecting sensitive organelles that govern critical cellular functions. The results showed that PTFE-MNPLs caused pronounced mitochondrial ultrastructural alterations in intestinal epithelial cells, including swelling, cristae disruption, and membrane damage, indicative of mitochondrial dysfunction (Fig. 7A–C). Mitochondrial membrane potential (MMP) measurements showed significant depolarization after 48 h at 200 µg/mL for both PTFE sizes in monocultures, but only PTFE-NPLs affected the barrier model

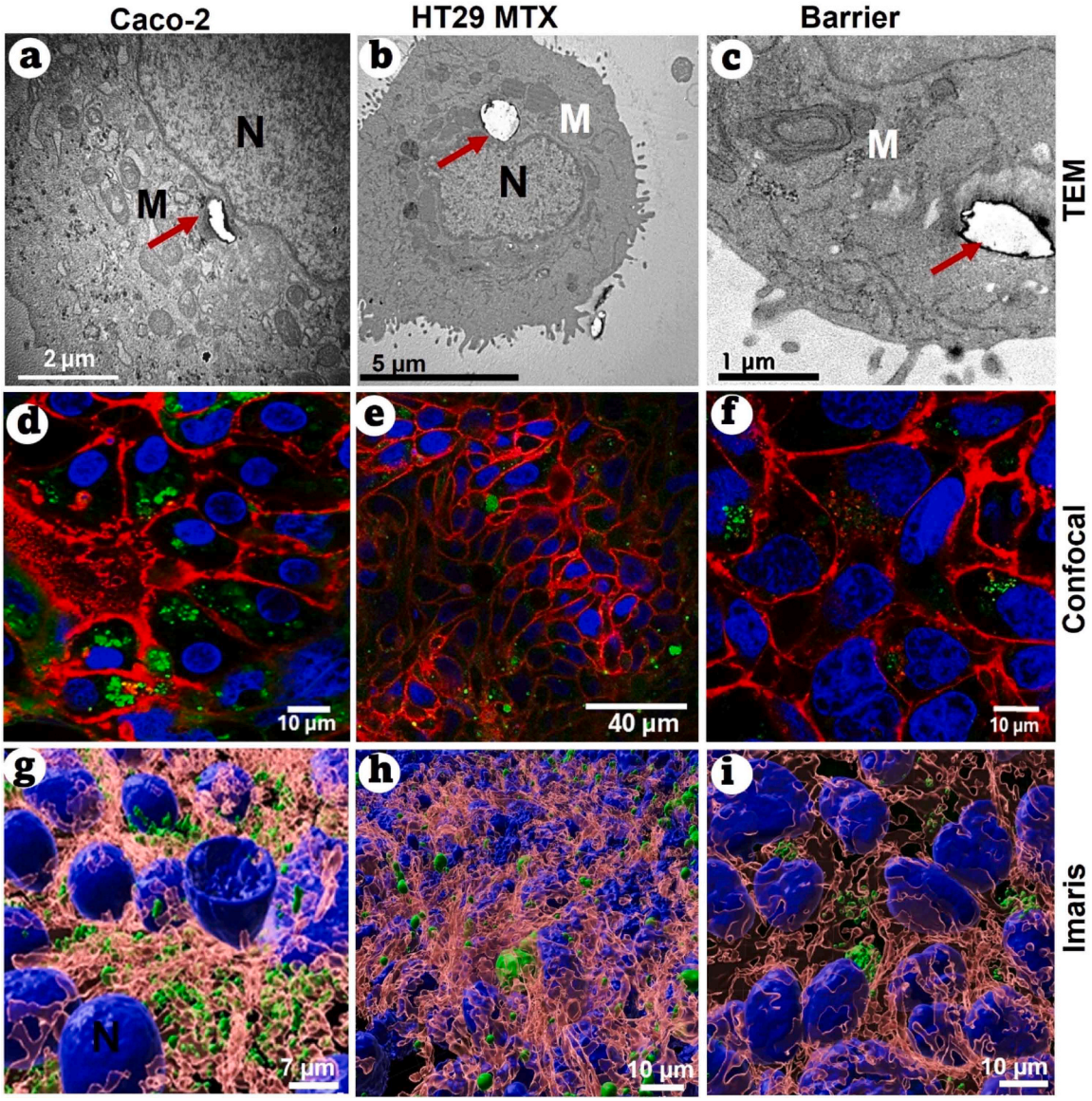

Fig. 4. Internalization of PTFE-MPLs (~2 µm) after 48 h exposure in intestinal epithelial models. TEM images (a–c) depict PTFE-MPL uptake in Caco-2 cells (a), HT29-MTX cells (b), and the Caco-2/HT29-MTX co-culture barrier (c). Red arrows highlight endocytosed PTFE-MPLs in various cellular compartments. (N) indicates the nucleus; (M) indicates mitochondria. Confocal microscopy (d–i) confirms intracellular localization of PTFE-MPLs (green), while 3D Imaris reconstructions (g–i) of the confocal images visualize their spatial distribution.

(Fig. 7A). TEM images revealed PTFE-NPLs inside mitochondria (Fig. 7B), forming large central vacuoles (Fig. 7C). Mitochondrial damage and excessive fission triggered mtDNA release, activating the cGAS-STING pathway and upregulating inflammatory factors (NLRP3, ASC, Caspase-1 p20, IL-1β) [47].

Multiple studies report that nanoplastic exposure disrupts mitochondrial function, decreases membrane potential, and induces oxidative stress, potentially leading to inflammation and apoptosis [48]. Xuan et al. [49] showed that PTFE-MNPL exposure impaired mitochondrial function and suppressed the AKT/mTOR pathway in murine intestinal organoids, resulting in reduced metabolic activity, autophagy, and necrosis. Fig. S2 illustrates how PTFE-NPLs internalize in Caco-2 or HT29-MTX monocultures, ultimately causing complete mitochondrial damage and cell apoptosis. Exposure to PS-NPLs activated the NLRP3 inflammasome in THP-1 cells, triggering IL-1β release, caspase-1 activation, and mitochondrial and lysosomal damage [50]. These events were accompanied by altered redox status, directly impacting mitochondria. Excessive reactive oxygen species disrupt antioxidant defence (e.g., CAT, SOD, GSTs, Cu/ZnSOD), causing inflammation, cell death, DNA and protein damage, lipid peroxidation, and mitochondrial dysfunction [51]. PS and PET nanoplastics elevate ROS, reduce mitochondrial membrane potential (ΔΨ), and increase Ca^{2+} in vitro [52,53]. These changes directly impair mitochondrial function and disrupt cellular homeostasis [54].

Oxidative stress is a primary initiator of hazardous molecular and cellular pathways, disrupting homeostasis and contributing to the development of various diseases. Our ROS measurements confirmed a concentration- and time-dependent increase, particularly at 48 h, for both PTFE-MPLs and NPLs (Fig. 8). Consistently, KC et al. [44] and Xuan et al. [49] demonstrated the capacity of PTFE-MNPLs to induce oxidative stress. Importantly, oxidative stress is not specific to a single material but is a common response associated with nearly all nanosized materials. Our previous studies have shown that the internalization of nanomaterials leads to oxidative stress and disturbances in antioxidant enzyme activity across various nanosized materials, including MNPLs [55–57]. Notably, the hazardous pathways, such as inflammation,

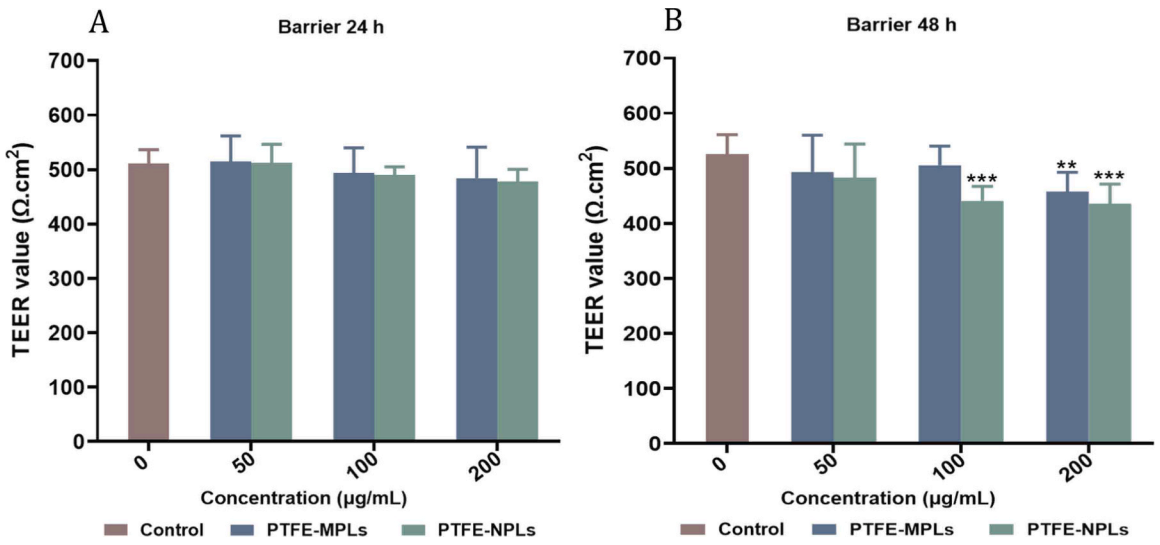

Fig. 5. TEER was measured in the differentiated Caco-2/HT29-MTX co-culture barrier. Cells were exposed to 0–200 µg/mL PTFE-MPLs and PTFE-NPLs for 24 h (A) and 48 h (B). Data are shown as mean ± SEM. Statistical analysis was performed using one-way ANOVA with Dunnett's post-test. $^{*}P \leq 0.05$, $^{**}P \leq 0.01$, $^{***}P \leq 0.001$.

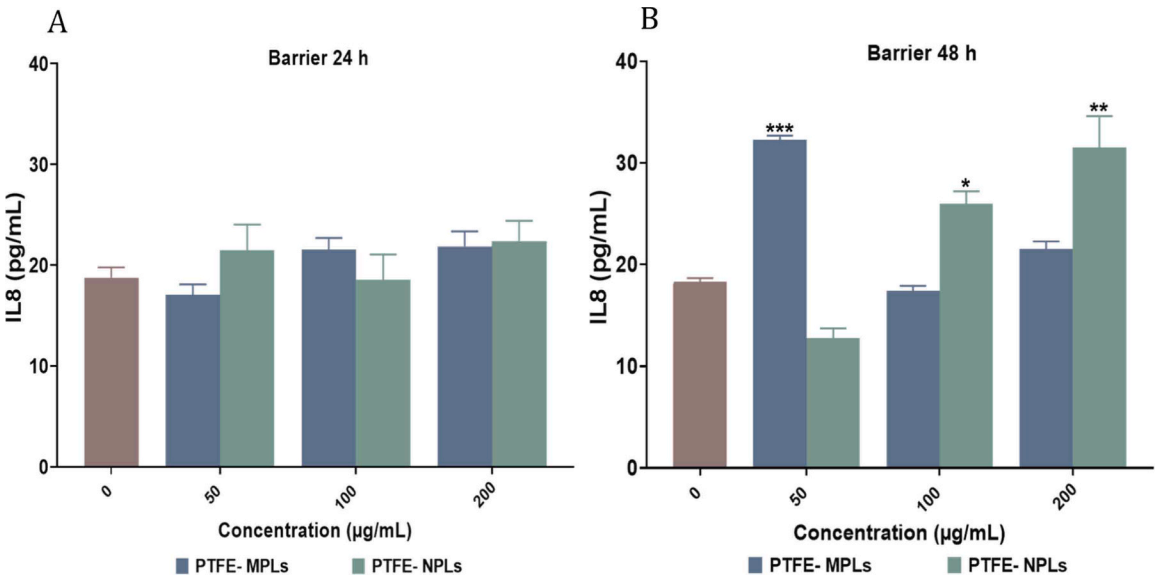

Fig. 6. Inflammatory effect of PTFE-MNPLs at different concentrations (0, 50, 100, and 200 µg/mL) on Caco-2/HT29-MTX co-culture (intestinal barrier). IL-8 release was measured after 24 h (A) and 48 h (B) of apical exposure. Data are represented as mean ± SEM and analysed using one-way ANOVA with Dunnett's post-test. $^{*}P \leq 0.05$, $^{**}P \leq 0.01$, $^{***}P \leq 0.001$.

disrupted cellular functions, impaired mitochondrial stability, and apoptosis, are primarily driven by micro- and nanoplastic accumulation. This accumulation ultimately results in oxidative stress and DNA damage [58]. Thus, these findings underscore the hazardous impacts of PTFE-MNPL exposure, emphasizing health risks that have not been sufficiently recognized.

3.7. Genotoxic and oxidative DNA damage

Exposure to hazardous materials can trigger cascades of cellular changes, ultimately leading to genotoxic effects from unrepaired DNA damage. PTFE-MNPLs demonstrated genotoxic potential in both undifferentiated and barrier-forming Caco-2 and HT29-MTX cells, with TEM and confocal imaging revealing their proximity to the nuclear envelope. DNA strand breaks increased significantly in all cell types at 24 and 48 h, particularly in Caco-2 cells. PTFE-NPLs induced greater damage than PTFE-MPLs, indicating a clear size-dependent effect (Fig. 9A). DNA damage also depended on the exposure time and dose of PTFE-MNPLs. FPG-modified comet assays in differentiated co-cultures confirmed oxidative DNA lesions, which rose from 15 to 20 % at 24 h to 22–30 % at 48 h for PTFE-MPLs and NPLs, demonstrating time- and size-dependent oxidative DNA damage (Fig. 9B). While most genotoxic effects were direct DNA breaks induced by PTFE-MNPLs, significant oxidative damage was also observed. Fig. 9C shows the degree of DNA damage in PTFE-MNPLs–exposed cells compared with non-exposed controls.

The high surface reactivity and efficient cellular uptake of MNPLs enhance interactions with mitochondria and nuclei, potentially interfering with DNA repair, promoting oxidative imbalance, and increasing chromosomal instability [59]. To date, no studies specifically address the genotoxic effects of PTFE-MNPL exposure [25]. Thus, comprehensive studies investigating their genotoxicity are urgently needed. Alarmingly, PTFE-MNPLs pose potential human health risks, as they

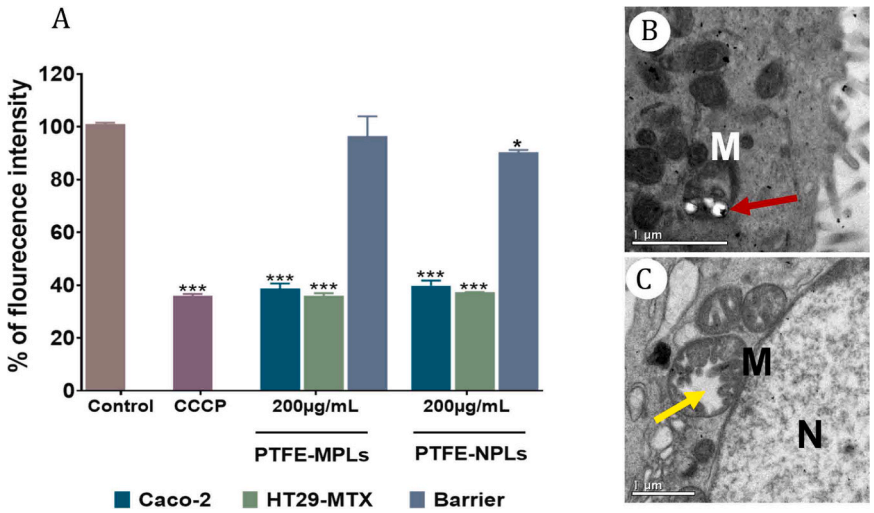

Fig. 7. Mitochondrial membrane potential was assessed in Caco-2, HT29-MTX, and Caco-2/HT29-MTX co-cultures after exposure to 200 µg/mL PTFE-MNPLs (A). TEM images show PTFE-NPLs inside mitochondria (B) and mitochondrial swelling (C). (N) indicates the nucleus; (M) indicates mitochondria. Red arrow indicates PTFE-NPLs inside mitochondria, and yellow arrow indicates mitochondrial vacuoles. Data are presented as mean ± SEM and analysed by two-way ANOVA with Tukey's post-test. *$P \leq 0.05$, ** $P \leq 0.01$, and ***$P \leq 0.001$.

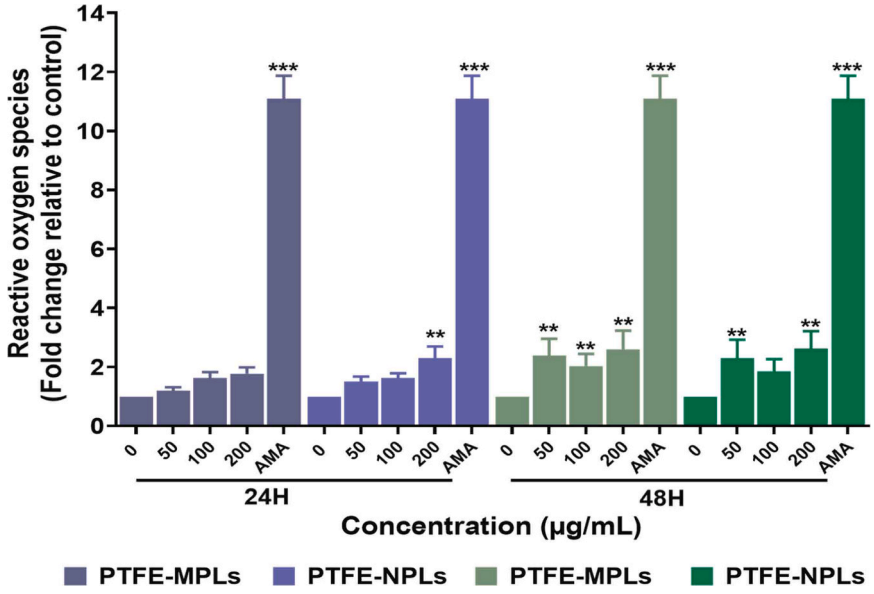

Fig. 8. Intracellular reactive oxygen species (ROS) production was measured in the differentiated Caco-2/HT29-MTX co-culture barrier after 24 or 48 h exposure to PTFE-MNPLs (0–200 µg/mL). Data are presented as mean ± SEM and analysed by two-way ANOVA with Tukey's post-test. *$P \leq 0.05$, **$P \leq 0.01$ and ***$P \leq 0.001$.

have already been detected in various human organs and bodily fluids alongside other microplastics [60–68]. Notably, the genotoxicity of nanoplastics released from real plastic containers has been investigated recently. Alaraby et al. [69] demonstrated that metal-doped nanoplastics originating from commercial products, such as milk plastic bottles, exhibit genotoxic effects.

Overall, evidence suggests that millions of particles can be released from PTFE-based utensils commonly used in everyday food preparation. Studies demonstrating the presence of PTFE in human tissues and bodily fluids, together with our findings on the hazardous effects of micro- and nanoplastic PTFE particles, highlight the urgent need for systematic risk assessments at multiple levels. Raising awareness among committees and stakeholders about the health risks linked to the improper use of plastics, especially PTFE-based products, is of critical importance. Furthermore, urgent and comprehensive research is needed to investigate the diverse toxic effects of PTFE-MNPLs, elucidate the underlying molecular mechanisms, and identify the cellular pathways involved. Future research should also prioritize the development of safer alternatives to mitigate potential human health risks associated with PTFE exposure.

4. Conclusion

The current study employed a physiologically relevant intestinal co-culture model (Caco-2/HT29-MTX), mimicking the human intestinal barrier to systematically evaluate the impacts of polytetrafluoroethylene micro/nanoplastics (PTFE-MNPLs). PTFE-MNPLs, regardless of size and particularly at the nanoscale, readily entered both differentiated and undifferentiated intestinal epithelial cells. These particles interacted with the nuclear membrane and mitochondria, causing structural and physiological disturbances. Inflammation and mitochondrial damage emerged as key hazards. They also induced significant oxidative stress

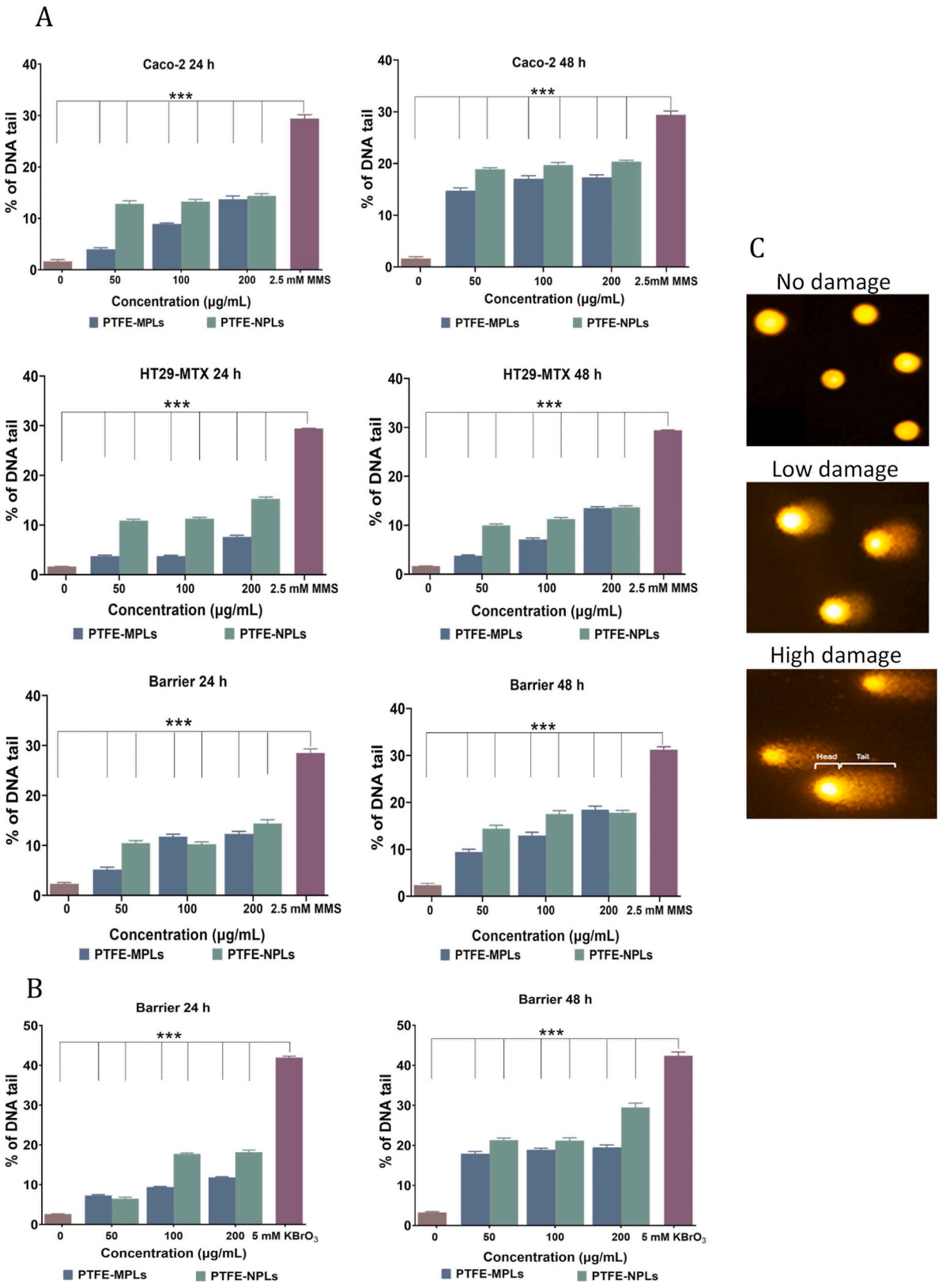

Fig. 9. Genotoxicity and oxidative DNA damage were assessed in cells after 24 and 48 h exposure to PTFE-MNPLs (0–200 µg/mL). Genotoxicity in undifferentiated Caco-2 and HT29-MTX monocultures, and in differentiated Caco-2/HT29-MTX co-cultures, is shown in panel (A). Oxidative damage in differentiated Caco-2/HT29-MTX co-cultures (B) was assessed using the FPG enzyme to distinguish direct DNA breaks from those resulting from oxidized DNA bases. Positive controls were 2.5 mM MMS and 5 mM $KBrO_3$. Representative fluorescent images of DNA damage are shown in (C). Data are presented as mean ± SEM and analysed by one-way ANOVA with Dunnett's post-test. $^{***}P \leq 0.001$.

and genotoxicity. Importantly, these effects were dependent on particle size, dose, and duration of exposure. Despite these impacts, PTFE-MNPLs did not significantly reduce cell viability, highlighting the subtle yet biologically significant risks. They can disrupt cellular homeostasis and alter the normal molecular and cellular microenvironment. These results challenge the long-standing assumption that PTFE particles are biologically inert. Their hazards appear to arise from both physical interactions and biochemical responses. The co-culture model closely reflects human intestinal physiology, strengthening the relevance of the findings. PTFE safety in food-contact applications should be reassessed. Future studies should focus on chronic, low-dose exposure using *in vivo* models to identify the specific pathways affected by PTFE-MNPLs. Particle size, persistence, and bioactivity should be considered when evaluating exposure risks.

Environmental implication

Polytetrafluoroethylene (PTFE) degrades into micro- and nanoplastics (MNPLs) which accumulate in the environment and affect humans through non-stick cookware exposure, among others. Using physiologically relevant intestinal cell models, mimicking the intestinal barrier, we show that both nanosized and microsized PTFE particles internalized into cells, inducing oxidative stress, DNA damage, and immune responses without immediate cytotoxicity. Our findings, under environmentally relevant concentrations and exposure durations, highlight the potential risks of PTFE-MNPLs to human health, underscoring the importance of evaluating environmental release, long-term exposure, and regulatory measures for these persistent plastic particles.

Funding

This study has received funding from the European Union's Horizon 2020 research and innovation programme under grant agreement No 965196. This work was partially supported by the Spanish Ministry of Science and Innovation (PID2020–116789RB-C43) and the Generalitat de Catalunya (2021-SGR-00731).

CRediT authorship contribution statement

Irene Barguilla: Writing – review & editing, Supervision, Conceptualization. **Elham Farghal Elkady:** Resources, Validation. **Ricard Marcos:** Writing – review & editing, Supervision, Conceptualization. **Alba Hernández:** Writing – review & editing, Supervision, Funding acquisition, Conceptualization. **Alba García-Rodríguez:** Writing – review & editing, Supervision, Conceptualization. **Doaa Abass:** Writing – original draft, Investigation, Conceptualization. **Mohamed Alaraby:** Writing – original draft, Supervision, Methodology, Conceptualization. **Michelle Morataya-Reyes:** Investigation, Data curation. **Gooya Banaei:** Methodology. **Joan Martín-Pérez:** Methodology, Investigation. **Laura Rubio:** Supervision, Investigation.

Declaration of Competing Interest

The authors declare that they have no known competing financial interests or personal relationships that could have appeared to influence the work reported in this paper.

Acknowledgment

Doaa Abass visiting researcher (2022–2024). A García-Rodríguez and M. Alaraby received funding from the postdoctoral program Beatriu de Pinós (Departament de Recerca i Universitats de la Generalitat de Catalunya, expedient: 2020 BP 00027 and 2022 BP 00026, respectively). L. Rubio and A. García-Rodríguez were granted with a Pre-Competitiu Project (PPC-24) from Universitat Autònoma de Barcelona. A. Hernández was granted an ICREA ACADEMIA award.

Appendix A. Supporting information

Supplementary data associated with this article can be found in the online version at doi:10.1016/j.jhazmat.2025.140255.

Data availability

Data will be made available on request.

References

[1] Jiao, H., Ali, S.S., Alsharbaty, M.H.M., Elsamahy, T., Abdelkarim, E., Schagerl, M., Al-Tohamy, R., Sun, J., 2024. A critical review on plastic waste life cycle assessment and management: challenges, research gaps, and future perspectives. J Ecotoxicol Environ Saf 271, 115942. https://doi.org/10.1016/j.ecoenv.2024.115942.

[2] Zhou, C., Ran, M., Wang, Z., Li, M., Wang, X., Zhang, C., Song, Z., 2025. Baseline biomonitoring of microplastic pollution in freshwater fish from the Chishui River, China: Insights into accumulation patterns and influencing factors. J Hazard Mater 495, 139055. https://doi.org/10.1016/j.jhazmat.2025.139055.

[3] Alaraby, M., Abass, D., Velázquez, A., Hernández, A., Marcos, R., 2025. New insights into the reproductive hazards posed by polystyrene nanoplastics. J Hazard Mater 492, 138210. https://doi.org/10.1016/j.jhazmat.2025.138210.

[4] Xia, Y., Wang, W.X., 2025. Subcellular toxicity assessments of microplastics released from food containers. J Hazard Mater 489, 137541. https://doi.org/10.1016/j.jhazmat.2025.137541.

[5] Cole, M., Gomiero, A., Jaén-Gil, A., Haave, M., Lusher, A., 2024. Microplastic and PTFE contamination of food from cookware. Sci Total Environ 929, 172577. https://doi.org/10.1016/j.scitotenv.2024.172577.

[6] Dhanumalayan, E., Joshi, G.M., 2018. Performance properties and applications of polytetrafluoroethylene (PTFE)—a review. Adv Compos Hybrid Mater 1 (2), 247–268. https://doi.org/10.1007/s42114-018-0023-8.

[7] Puts, G.J., Crouse, P., Ameduri, B.M., 2019. Polytetrafluoroethylene: synthesis and characterization of the original extreme polymer. Chem Rev 119 (3), 1763–1805. https://doi.org/10.1021/acs.chemrev.8b00458.

[8] Luo, Y., Gibson, C.T., Chuah, C., Tang, Y., Naidu, R., Fang, C., 2022. Raman imaging for the identification of Teflon microplastics and nanoplastics released from non-stick cookware. Sci Total Environ 851, 158293. https://doi.org/10.1016/j.scitotenv.2022.158293.

[9] Snekkevik, V.K., Cole, M., Gomiero, A., Haave, M., Khan, F.R., Lusher, A.L., 2024. Beyond the food on your plate: investigating sources of microplastic contamination in home kitchens. Heliyon 10 (15), e35022. https://doi.org/10.1016/j.heliyon.2024.e35022.

[10] Campos, A.R.A., Luza, K.M.B., Subebe, M.J.B., Tabelin, C.B., Phengsaart, T., Arima, T., Seno, R., Butalid, R., Escabarte, A.B., Mazahery, A.R.F., Coyoca, G.S.E., Villacorte-Tabelin, M., 2025. Polytetrafluoroethylene (PTFE) microplastics affect angiogenesis and central nervous system (CNS) development of duck embryo. Emerg Contam 11 (1), 100433. https://doi.org/10.1016/j.emcon.2024.100433.

[11] Khaliq, Z., Ashraf, M.B., Abbasi, N.A., Ahmad, S.R., Shahid, S.U., Qadir, A., 2024. Assessment of microplastics in gastrointestinal tract of cattle egret (*Bubulcus ibis*) from a metropolitan city Lahore, Pakistan. Environ Sci Pollut Res 31 (56), 64903–64912. https://doi.org/10.1007/s11356-024-35540-8.

[12] Alaraby, M., Abass, D., Velázquez, A., Hernández, A., Marcos, R., 2025. Occurrence, analysis, and toxicity of polyethylene terephthalate microplastics: a review. Environ Chem Lett 23, 1025–1059. https://doi.org/10.1007/s10311-025-01841-8.

[13] Nihart, A.J., Garcia, M.A., El Hayek, E., Liu, R., Olewine, M., Kingston, J.D., Castillo, E.F., Gullapalli, R.R., Howard, T., Bleske, B., Scott, J., Gonzalez-Estrella, J., Gross, J.M., Spilde, M., Adolphi, N.L., Gallego, D.F., Jarrell, H.S., Dvorscak, G., Zuluaga-Ruiz, M.E., West, A.B., Campen, M.J., 2025. Bioaccumulation of microplastics in decedent human brains. Nat Med 31 (4), 1114–1119. https://doi.org/10.1038/s41591-024-03453-1.

[14] Rocabert, A., Martín-Pérez, J., Pareras, L., Egea, R., Alaraby, M., Cabrera-Gumbau, J.M., Sarmiento, I., Martínez-Urtaza, J., Rubio, L., Barguilla, I., Marcos, R., García-Rodríguez, A., Hernández, A., 2025. Nanoplastic exposure affects the intestinal microbiota of adult *Drosophila* flies. Sci Total Environ 980, 179545. https://doi.org/10.1016/j.scitotenv.2025.179545.

[15] Marcellus, K.A., Prescott, D., Scur, M., Ross, N., Gill, S.S., 2025. Exposure of polystyrene nano- and microplastics in increasingly complex *in vitro* intestinal cell models. Nanomaterials 15 (4), 267. https://doi.org/10.3390/nano15040267.

[16] Hsu, W.H., Chen, Y.Z., Chiang, Y.T., Chang, Y.T., Wang, Y.W., Hsu, K.T., Hsu, Y.Y., Wu, P.T., Lee, B.H., 2025. Polystyrene nanoplastics disrupt the intestinal microenvironment by altering bacteria-host interactions through extracellular vesicle-delivered microRNAs. Nat Commun 16 (1), 5026. https://doi.org/10.1038/s41467-025-59884-y.

[17] Kutralam-Muniasamy, G., Shruti, V.C., Pérez-Guevara, F., Garcia, B.D.G., 2025. Unraveling microplastic behavior in simulated digestion: methods, insights, and standardization. J Hazard Mater 493, 138340. https://doi.org/10.1016/j.jhazmat.2025.138340.

[18] Herrala, M., Huovinen, M., Järvelä, E., Hellman, J., Tolonen, P., Lahtela-Kakkonen, M., Rysä, J., 2023. Micro-sized polyethylene particles affect cell viability and oxidative stress responses in human colorectal adenocarcinoma Caco-

2 and HT-29 cells. Sci Total Environ 867, 161512. https://doi.org/10.1016/j.scitotenv.2023.161512.
[19] Jin, T., Liu, Y., Lyu, H., He, Y., Sun, H., Tang, J., Xing, B., 2024. Plastic takeaway food containers may cause human intestinal damage in routine life usage: microplastics formation and cytotoxic effect. J Hazard Mater 475, 134866. https://doi.org/10.1016/j.jhazmat.2024.134866.
[20] Janiga-MacNelly, A., Hoang, T.C., Lavado, R., 2025. Comparative toxicity of microplastics obtained from human consumer products on human cell-based models. Food Chem Toxicol 196, 115194. https://doi.org/10.1016/j.fct.2024.115194.
[21] Banaei, G., García-Rodríguez, A., Tavakolpournegari, A., Martín-Pérez, J., Villacorta, A., Marcos, R., Hernández, A., 2023. The release of polylactic acid nanoplastics (PLA-NPLs) from commercial teabags: obtention, characterization, and hazard effects of true-to-life PLA-NPLs. J Hazard Mater 458, 131899. https://doi.org/10.1016/j.jhazmat.2023.131899.
[22] Villacorta, A., Cazorla-Ares, C., Fuentes-Cebrian, V., Valido, I.H., Vela, L., Carrillo-Navarrete, F., Morataya-Reyes, M., Mejia-Carmona, K., Pastor, S., Velázquez, A., Arribas Arranz, J., Marcos, R., López-Mesas, M., Hernández, A., 2024. Fluorescent labeling of micro/nanoplastics for biological applications with a focus on "true-to-life" tracking. J Hazard Mater 476, 135134. https://doi.org/10.1016/j.jhazmat.2024.135134.
[23] Kameníková, E., Hrušková, A., Udrea, C., Bojan, M., Palovčík, J., Solný, T., Šudomová, L., Vojtová, L., Brtnický, M., Kučerík, J., 2025. Testing laboratory protocols for micro- and nano-PET particles preparation by bottom-up chemical and top-down physical methods and implications for environmental studies. Environ Monit Assess 197 (10), 1120. https://doi.org/10.1007/s10661-025-14582-6.
[24] Prasad, R.Y., Wallace, K., Daniel, K.M., Tennant, A.H., Zucker, R.M., Strickland, J., Dreher, K., Kligerman, A.D., Blackman, C.F., DeMarini, D.M., 2013. Effect of treatment media on the agglomeration of titanium dioxide nanoparticles: impact on genotoxicity, cellular interaction, and cell cycle. ACS Nano 7 (3), 1929–1942. https://doi.org/10.1021/nn302280n.
[25] Alaraby, M., Abass, D., Velázquez, A., Hernández, A., Marcos, R., 2025. Polytetrafluoroethylene microplastics properties, pollution, toxicity and analysis: a review. Environ Chem Lett. https://doi.org/10.1007/s10311-025-01885-w. Published on line.
[26] Lee, S., Kang, K.K., Sung, S.E., Choi, J.H., Sung, M., Seong, K.Y., Lee, J., Kang, S., Yang, S.Y., Lee, S., Lee, K.R., 2022. *In vivo* toxicity and pharmacokinetics of polytetrafluoroethylene microplastics in ICR mice. Polymers 14 (11), 2220. https://doi.org/10.3390/polym14112220.
[27] Chelomin, V.P., Slobodskova, V.V., Kukla, S.P., Mazur, A.A., Dovzhenko, N.V., Zhukovskaya, A.F., Karpenko, A.A., Karpenko, M.A., Odintsov, V.S., 2023. Dietary exposure to particles of polytetrafluoroethylene (PTFE) and polymethylmethacrylate (PMMA) induces different responses in periwinkles *Littorina brevicula*. Int J Mol Sci 24 (9), 8243. https://doi.org/10.3390/ijms24098243.
[28] Stock, V., Laurisch, C., Franke, J., Dönmez, M.H., Voss, L., Böhmert, L., Braeuning, A., Sieg, H., 2021. Uptake and cellular effects of PE, PP, PET and PVC microplastic particles. Toxicol Vitr 70, 105021. https://doi.org/10.1016/j.tiv.2020.105021.
[29] Alaraby, M., Villacorta, A., Abass, D., Hernández, A., Marcos, R., 2023. The hazardous impact of true-to-life PET nanoplastics in *Drosophila*. Sci Total Environ 863, 160954. https://doi.org/10.1016/j.scitotenv.2022.160954.
[30] Alaraby, M., Abass, D., Farre, M., Hernández, A., Marcos, R., 2024. Are bioplastics safe? Hazardous effects of polylactic acid (PLA) nanoplastics in *Drosophila*. Sci Total Environ 919, 170592. https://doi.org/10.1016/j.scitotenv.2024.170592.
[31] Domenech, J., Villacorta, A., Ferrer, J.F., Llorens-Chiralt, R., Marcos, R., Hernández, A., Catalán, J., 2024. *In vitro* cell-transforming potential of secondary polyethylene terephthalate and polylactic acid nanoplastics. J Hazard Mater 469, 134030. https://doi.org/10.1016/j.jhazmat.2024.134030.
[32] Eliso, M.C., Billè, B., Cappello, T., Maisano, M., 2024. Polystyrene micro- and nanoplastics (PS MNPs): a review of recent advances in the use of -omics in PS MNP toxicity studies on aquatic organisms. Fishes 9 (3), 98. https://doi.org/10.3390/fishes9030098.
[33] Alaraby, M., Abass, D., Domenech, J., Hernández, A., Marcos, R., 2022. Hazard assessment of ingested polystyrene nanoplastics in *Drosophila* larvae. Environ Sci Nano 9 (5), 1845–1857. https://doi.org/10.1039/D1EN01199E.
[34] Cortés, C., Domenech, J., Salazar, M., Pastor, S., Marcos, R., Hernández, A., 2020. Nanoplastics as a potential environmental health factor: effects of polystyrene nanoparticles on human intestinal epithelial Caco-2 cells. Environ Sci Nano 7 (1), 272–285. https://doi.org/10.1039/C9EN00523D.
[35] Ji, Y., Chen, L., Wang, Y., Zhang, J., Yu, Y., Wang, M., Wang, X., Liu, W., Yan, B., Xiao, L., Song, X., Lv, C., Chen, L., 2024. Realistic nanoplastics induced pulmonary damage via the crosstalk of ferritinophagy and mitochondrial dysfunction. ACS Nano 18 (26), 16790–16807. https://doi.org/10.1021/acsnano.4c02335.
[36] García-Rodríguez, A., Vila, L., Cortés, C., Hernández, A., Marcos, R., 2018. Effects of differently shaped TiO_2NPs (nanospheres, nanorods and nanowires) on the *in vitro* model (Caco-2/HT29) of the intestinal barrier. Part Fibre Toxicol, 15 (1), 33. https://doi.org/10.1186/s12989-018-0269-x.
[37] Alaraby, M., Hernández, A., Annangi, B., Demir, E., Bach, J., Rubio, L., Creus, A., Marcos, R., 2015. Antioxidant and antigenotoxic properties of CeO_2 NPs and cerium sulphate: studies with *Drosophila melanogaster* as a promising. vivo Model Nanotoxicology 9 (6), 749–759. https://doi.org/10.3109/17435390.2014.976284.
[38] Stock, V., Böhmert, L., Lisicki, E., Block, R., Cara-Carmona, J., Kim Pack, L., Selb, R., Lichtenstein, D., Voss, L., Henderson, C.J., Zabinsky, E., Sieg, H., Braeuning, A., Lampen, A., 2019. Uptake and effects of orally ingested polystyrene microplastic particles *in vitro* and *in vivo*. Arch Toxicol 93, 1817–1833. https://doi.org/10.1007/s00204-019-02478-7.
[39] González, I.T., Saenen, N.D., Van Belleghem, F., Smeets, K., 2025. Polystyrene microplastics of varying sizes affect cell mechanisms depending on their uptake and weathering profile in Caco-2/HT29-MTX-E12 coculture. Toxicol Lett 411, S255. https://doi.org/10.1016/j.toxlet.2025.07.603.
[40] García-Rodríguez, A., Gutiérrez, J., Villacorta, A., Arribas Arranz, J., Romero-Andrada, I., Lacoma, A., Marcos, R., Hernández, A., Rubio, L., 2024. Polylactic acid nanoplastics (PLA-NPLs) induce adverse effects on an *in vitro* model of the human lung epithelium: the Calu-3 air-liquid interface (ALI) barrier. J Hazard Mater 475, 134900. https://doi.org/10.1016/j.jhazmat.2024.134900.
[41] Zou, X., Pan, M., Liu, Y., Wang, S., Xu, H., Chu, X., 2025. Effects of co-exposure to microplastics and perfluorooctanoic acid on the Caco-2 cells. Toxicology 515, 154152. https://doi.org/10.1016/j.tox.2025.154152.
[42] Yu, S., He, J., Xie, K., 2023. Zonula occludens proteins signaling in inflammation and tumorigenesis. Int J Biol Sci 19 (12), 3804. https://doi.org/10.7150/ijbs.85765.
[43] Chen, X., Xuan, Y., Chen, Y., Yang, F., Zhu, M., Xu, J., Chen, J., 2024. Polystyrene nanoplastics induce intestinal and hepatic inflammation through activation of NF-κB/NLRP3 pathways and related gut-liver axis in mice. Sci Total Environ 935, 173458. https://doi.org/10.1016/j.scitotenv.2024.173458.
[44] KC, P.B., Maharjan, A., Acharya, M., Lee, D., Kusma, S., Gautam, R., Kwon, J.T., Kim, C., Kim, K., Kim, H., Heo, Y., 2023. Polytetrafluorethylene microplastic particles mediated oxidative stress, inflammation, and intracellular signaling pathway alteration in human derived cell lines. Sci Total Environ 897, 165295. https://doi.org/10.1016/j.scitotenv.2023.165295.
[45] Jo, J., Acharya, M., KC, P.B., Maharjan, A., Lee, D., Gautam, R., Kwon, J.T., Kim, K., Kim, C., Heo, Y., Kim, H., 2023. Immunodysregulatory potentials of polyethylene or polytetrafluorethylene microplastics to mice subacutely exposed via intragastric intubation. Toxicol Res 39 (3), 419–427. https://doi.org/10.1007/s43188-023-00172-6.
[46] Mahmud, F., Sarker, D.B., Jocelyn, J.A., Sang, Q.X.A., 2024. Molecular and cellular effects of microplastics and nanoplastics: focus on inflammation and senescence. Cells 13 (21), 1788. https://doi.org/10.3390/cells13211788.
[47] Zhao, M., Xie, J., Zhang, J., Zhao, B., Zhang, Y., Xue, J., Zhang, R., Zhang, R., Wang, H., Li, Y., Ge, W., Zhou, X., 2024. Disturbance of mitochondrial dynamics led to spermatogenesis disorder in mice exposed to polystyrene micro- and nanoplastics. Environ Pollut 362, 124935. https://doi.org/10.1016/j.envpol.2024.124935.
[48] Siemiątkowska, B., Szczepanowska, J., 2025. Mitochondrial stress response in lung cells triggered by the inhaled nanoplastics. Arch Toxicol (Online Print). https://doi.org/10.1007/s00204-025-04194-x.
[49] Xuan, L., Luo, J., Qu, C., Guo, P., Yi, W., Yang, J., Yan, Y., Guan, H., Zhou, P., Huang, R., 2024. Predictive metabolomic signatures for safety assessment of three plastic nanoparticles using intestinal organoids. Sci Total Environ 913, 169606. https://doi.org/10.1016/j.scitotenv.2023.169606.
[50] Laganà, A., Visalli, G., Facciolà, A., Saija, C., Bertuccio, M.P., Baluce, B., Celesti, C., Iannazzo, D., Di Pietro, A., 2024. Sterile inflammation induced by respirable micro and nano polystyrene particles in the pathogenesis of pulmonary diseases. Toxicol Res 13(5) tfae138. https://doi.org/10.1093/toxres/tfae138.
[51] Kıran, T.R., Otlu, O., Karabulut, A.B., 2023. Oxidative stress and antioxidants in health and disease. J Lab Med 47 (1), 1–11. https://doi.org/10.1515/labmed-2022-0108.
[52] Xuan, L., Wang, Y., Qu, C., Yan, Y., Yi, W., Yang, J., Skonieczna, M., Chen, C., Miszczyk, J., Ivanov, D.S., Zakaly, H.M.H., Markovic, V., Huang, R., 2023. Metabolomics reveals that PS-NPs promote lung injury by regulating prostaglandin B1 through the cGAS-STING pathway. Chemosphere 342, 140108. https://doi.org/10.1016/j.chemosphere.2023.140108.
[53] Annangi, B., Villacorta, A., Vela, L., Tavakolpournegari, A., Marcos, R., Hernández, A., 2023. Effects of true-to-life PET nanoplastics using primary human nasal epithelial cells. Environ Toxicol Pharm 100, 104140. https://doi.org/10.1016/j.etap.2023.104140.
[54] Aguilar-Guzmán, J.C., Bejtka, K., Fontana, M., Valsami-Jones, E., Villezcas, A.M., Vazquez-Duhalt, R., Rodríguez-Hernández, A.G., 2022. Polyethylene terephthalate nanoparticles effect on RAW 264.7 macrophage cells. Micro Nanoplast 2 (1), 9. https://doi.org/10.1186/s43591-022-00027-1.
[55] Alaraby, M., Hernández, A., Marcos, R., 2018. Systematic *in vivo* study of NiO nanowires and nanospheres: biodegradation, uptake and biological impacts. Nanotoxicology 12, 1027–1044. https://doi.org/10.1080/17435390.2018.1513091.
[56] Alaraby, M., Hernández, A., Marcos, R., 2021. Novel insights into biodegradation, interaction, internalization and impacts of high-aspect-ratio TiO_2 nanomaterials: a systematic *in vivo* study using *Drosophila melanogaster*. J Hazard Mater 409, 124474. https://doi.org/10.1016/j.jhazmat.2020.124474.
[57] Alaraby, M., Abass, D., Villacorta, A., Hernández, A., Marcos, R., 2022. Antagonistic *in vivo* interaction of polystyrene nanoplastics and silver compounds: a study using *Drosophila*. Sci Total Environ 842, 156923. https://doi.org/10.1016/j.scitotenv.2022.156923.
[58] Barría, C., Balasch, J.C., Brandts, I., Oliva, D., Iriarte, J.L., Teles, M., 2025. Immunological responses, oxidative stress, and histopathological effects of nanoplastics on commercially relevant mussel species: a review. J Hazard Mater Adv 17, 100540. https://doi.org/10.1016/j.hazadv.2024.100540.
[59] Płuciennik, K., Sicińska, P., Misztal, W., Bukowska, B., 2024. Important factors affecting induction of cell death, oxidative stress and DNA damage by nano- and microplastic particles *in vitro*. Cells 13 (9), 768. https://doi.org/10.3390/cells13090768.

[60] Liu, S., Liu, X., Guo, J., Yang, R., Wang, H., Sun, Y., Chen, B., Dong, R., 2022. The association between microplastics and microbiota in placentas and meconium: the first evidence in humans. Environ Sci Technol 57 (46), 17774–17785. https://doi.org/10.1021/acs.est.2c04706.

[61] Jenner, L.C., Rotchell, J.M., Bennett, R.T., Cowen, M., Tentzeris, V., Sadofsky, L.R., 2022. Detection of microplastics in human lung tissue using μFTIR spectroscopy. Sci Total Environ 831, 154907. https://doi.org/10.1016/j.scitotenv.2022.154907.

[62] Wang, S., Lu, W., Cao, Q., Tu, C., Zhong, C., Qiu, L., Li, S., Zhang, H., Lan, M., Qiu, L., Li, X., Liu, Y., Zhou, Y., Liu, J., 2023. Microplastics in the lung tissues associated with blood test index. Toxics 11 (9), 759. https://doi.org/10.3390/toxics11090759.

[63] Zhang, C., Zhang, G., Sun, K., Ren, J., Zhou, J., Liu, X., Lin, F., Yang, H., Cao, J., Nie, L., Zhang, P., Zhang, L., Wang, Z., Guo, H., Lin, X., Duan, S., Cao, J., Huang, H., 2024. Association of mixed exposure to microplastics with sperm dysfunction: a multi-site study in China. EBioMedicine 108, 105369. https://doi.org/10.1016/j.ebiom.2024.105369.

[64] Yun, X., Liang, L., Tian, J., Li, N., Chen, Z., Zheng, Y., Duan, S., Zhang, L., 2024. Raman-guided exploration of placental microplastic exposure: unraveling the polymeric tapestry and assessing developmental implications. J Hazard Mater 477, 135271. https://doi.org/10.1016/j.jhazmat.2024.135271.

[65] Rotchell, J.M., Austin, C., Chapman, E., Atherall, C.A., Liddle, C.R., Dunstan, T.S., Blackburn, B., Mead, A., Filart, K., Beeby, E., Cunningham, K., Allen, J., Draper, H., Guinn, B.-A., 2024. Microplastics in human urine: characterisation using μFTIR and sampling challenges using healthy donors and endometriosis participants. Ecotoxicol Environ Saf 274, 116208. https://doi.org/10.1016/j.ecoenv.2024.116208.

[66] Liu, S., Yang, Y., Du, Z., Wang, C., Li, L., Zhang, M., Ni, S., Yue, Z., Yang, K., Gao, H., Zeng, Y., Qin, Y., Li, J., Yin, C., Zhang, M., 2024. Percutaneous coronary intervention leads to microplastics entering the blood: interventional devices are a major source. J Hazard Mater 476, 135054. https://doi.org/10.1016/j.jhazmat.2024.135054.

[67] Tian, J., Liang, L., Li, Q., Li, N., Zhu, X., Zhang, L., 2025. Association between microplastics in human amniotic fluid and pregnancy outcomes: detection and characterization using Raman spectroscopy and pyrolysis GC/MS. J Hazard Mater 482, 136637. https://doi.org/10.1016/j.jhazmat.2024.136637.

[68] Zhang, L., Tian, J., Zhu, X., Wang, L., Yun, X., Liang, L., Duan, S., 2025. Cross-platform detection of microplastics in human biological tissues: comparing spectroscopic and chromatographic approaches. J Hazard Mater 492, 138133. https://doi.org/10.1016/j.jhazmat.2025.138133.

[69] Alaraby, M., Villacorta, A., Abass, D., Hernández, A., Marcos, R., 2024. Titanium-doped PET nanoplastics from opaque milk bottle degradation as a model of environmental true-to-life nanoplastics: hazardous effects on *Drosophila*. Environ Pollut 341, 122968. https://doi.org/10.1016/j.envpol.2023.122968.